Available online at www.sciencedirect.com

SciVerse ScienceDirect

Ceramics International 39 (2013) 3195–3204

CERAMICS INTERNATIONAL

www.elsevier.com/locate/ceramint

Effect of microwave sintering on the structural and densification behavior of sol–gel derived zirconia toughened alumina (ZTA) nanocomposites

R. Vasudevan[a,b], T. Karthik[c], S. Ganesan[b], R. Jayavel[a,*]

[a]Centre for Nanoscience and Technology, Anna University, Chennai 600025, India
[b]Department of Medical Physics, Anna University, Chennai 600025, India
[c]Department of Materials Science and Engineering, Indian Institute of Technology, Hyderabad 502205, India

Received 10 June 2012; received in revised form 2 October 2012; accepted 3 October 2012
Available online 11 October 2012

Abstract

Zirconia toughened alumina (ZTA) nanocomposites with different zirconia contents (5–20 mol%) were prepared by the sol–gel method. The prepared composites were sintered at 1300 °C by both conventional and microwave techniques. The crystallinity, average grain size, microstructure and densification of the samples prepared by conventional and microwave sintering methods were compared. X-ray diffraction analysis shows that the microwave sintered samples possess higher tetragonality and also exhibit reduced particle size compared to conventional sintering. HR-SEM surface micrograph reveals that the microwave sintered samples have homogeneous particle size distribution with less degree of porosity. TEM analysis confirms uniform distribution of particles with an average particle size of 20 nm for the microwave sintered sample. SAED pattern reveals that the microwave sintered samples possess improved crystallinity compared to conventional sintered samples. The apparent porosity and density of ZTA nanocomposites measured for different zirconia contents show that the densification of 97% could be achieved for the microwave sintered samples with higher content of zirconium.

Keywords: ZTA nanocomposites; Microwave sintering technique; Transformation toughening; HR-TEM

1. Introduction

The increasing interests in ceramic nanocomposites are due to their mechanical, thermal and chemical properties suitable for high temperature structural applications. Al_2O_3–ZrO_2 (ZTA) nanocomposites are well known structural ceramic material owing to their higher hardness, high elastic modulus, high fracture toughness, high strength and ductility, low wear resistance and chemical inertness [1–3]. ZTA nanocomposites are extensively used in structural engineering applications such as high efficiency gas turbines, aerospace and automotive components, corrosion and wear resistant coatings, bone joint cup and head of the bone, ceramic membranes in separation such as hyper-filtration, reverse osmosis, gas separation and catalytic and photocatalytic applications [1–3]. In ZTA nanocomposites, the strength and the toughness are improved by the stress-induced Martensitic t→m transformation of dispersed zirconia particles into the Al_2O_3 matrix [4–6]. The extent of densification and toughening achieved in ZTA nanocomposites depends on the size of Al_2O_3 and ZrO_2 particles, volume fraction of ZrO_2 retained in the metastable tetragonal phase at room temperature as well as the relative distribution of Al_2O_3 and ZrO_2 in the matrix. While a finer particle size of both Al_2O_3 and ZrO_2 not only enhances the chances of uniform distribution, it also increases the possibility of ZrO_2 being retained in the metastable tetragonal phase. The uniform particle size distribution of Al_2O_3 and ZrO_2 in ZTA nanocomposites is limited by the coarsening effect of dispersed zirconia particles [7]. In order to obtain homogeneous mixing of Al_2O_3 and ZrO_2 particles, the sol–gel technique has been adopted to

*Corresponding author. Tel.: +91 44 22359112; fax: +91 44 22301656.
E-mail address: rjvel@annauniv.edu (R. Jayavel).

0272-8842/$ - see front matter © 2012 Elsevier Ltd and Techna Group S.r.l. All rights reserved.
http://dx.doi.org/10.1016/j.ceramint.2012.10.004

prepare ZTA nanocomposites [8]. Other methods such as combustion, precipitation, mechanical milling, hydrothermal methods have also been used [9]. Among these the sol–gel method has many advantages as the synthesis is done at relatively lower temperature to obtain homogeneous composites with high purity [1]. A uniform particle shape with continuous and narrow size distribution is expected to yield products with reduced microstructural defects due to the improved powder flowability and better packing density [10].

In the high temperature conventional sintering process, densification and toughness of ZTA nanocomposites are limited by the inhomogeneous distribution of Al_2O_3 and ZrO_2 particles due to the rapid grain growth as well as the lower degree of metastable retention of t-phase at room temperature. During the stress-induced Martensitic t→m transformation, the monoclinic phase is more stable at room temperature and it is difficult to retain the metastable tetragonal phase in the conventional sintering due to its slow cooling process. Hence the existence of monoclinic phase affects the microstructural densification and mechanical behavior of the ZTA nanocomposites. Excessive grain growth makes it extremely difficult to obtain dense materials with nanometric grain size. In the conventional sintering, the densification and grain growth are driven by diffusion and hence it is difficult to realize the densification without promoting grain growth [11]. In order to overcome this problem, microwave sintering technique has been adopted due to its fast sintering action, in which the grain growth is effectively controlled and also higher degree of metastable tetragonal phase is retained at room temperature while the monoclinic phase is suppressed with the addition of zirconia particles [12–15]. In the conventional sintering process the radiant heat absorbed at the surface of the nanocomposites reaches the core by thermal conduction producing high temperature gradient and strain. In the microwave heating each constituent unit of the crystal lattice is excited to certain constant amplitude, which results in a highly uniform distribution of heat in the bulk of the material with reduced thermal strain [16].

In this investigation, a systematic approach has been made to study the effect of microwave sintering on the structural, microstructural and densification behavior of ZTA nanocomposites synthesized by the sol–gel technique with different zirconia content (5–20 mol%). The improved properties of ZTA nanocomposites with microwave sintering are compared with conventional sintering process.

2. Experimental procedure

(i) *Synthesis of ZTA nanopowders*

Aqueous solutions of $Al(NO_3)_3 \cdot 9H_2O$ and $ZrOCl_2 \cdot 8H_2O$ were used as the source for Al_2O_3 and ZrO_2. Initially 0.5 M of $Al(NO_3)_3 \cdot 9H_2O$ and $ZrOCl_2 \cdot 8H_2O$ solutions were prepared separately with 2-methoxy ethanol as a solvent. The prepared solutions were mixed and continuously stirred for several hours at room temperature until it turned into a yellowish sol. Simultaneously the solutions of $Al_2O_{3-x}ZrO_2$ (where $x=5,10,15$ and 20 mol%) were prepared. Then the stabilized sol was kept for aging until it becomes a transparent viscous gel. The aged gel of each composition was washed repeatedly with methoxy–ethanol solvent to remove chloride and nitrate ions present in the material and finally the gel was dried at 120 °C for overnight. Thus the initial precursor powder was synthesized by the sol–gel route, further in order to study the sintering effect, the ZTA as-prepared powders were sintered by both conventional and microwave sintering techniques as follows.

(ii) *Sintering of nanopowders*

Initially the dried powders were pre-sintered at 600 °C to remove the organic and other residues present in the material and then ground into fine mixing by both sintering techniques. Further the pre-sintered powder was mixed with 2 wt% of PVA binder and then cylindrical pellets were uniaxially compacted at a pressure of 4 tones for 3 min.

The prepared pellets were subjected to both conventional and microwave sintering processes. In the conventional sintering the samples were heated to 1300 °C at a rate of 5 °C/min and homogenized for 2 h in air atmosphere and then cooled down to room temperature at the same rate. Microwave sintering was performed by using VBCC 2-magnetron microwave heating furnace in which the material was heating up to 1300 °C at a rate of 50 °C/min and soaked for 20 min followed by fast cooling to room temperature at a rate of 20 °C/min. The temperature was measured with a pyrometer and it was calibrated with reference to thermocouple; also the emissivity value was measured between 0.90 and 0.98 for the different contents of zirconia. The output power level of the microwave is about 2.2 KW with 2.45 GHz frequency and it was controlled by Eurotherm PID controller but for the conventional furnace it is 3.8 KW. As compared to the conventional sintering, the microwave sintering is required only for an output power of about 2.2 KW to sinter the material even in the elevated temperatures of about 1300 °C or more. Hence it has an advantage of lower power consumption with high energy as well as minimal thermal stress in the material during sintering at higher temperature which leads to better material stability. The different heating and cooling rates were employed for conventional and microwave sintering techniques. When the material was sintered with the microwave technique, because of its fast heating and cooling rates by which it could retain the large fraction of finer t-ZrO_2 crystallites than the larger m-ZrO_2 phases it would lead to better microstructure as well as improved densification of the material. Vice versa during the conventional sintering, the high ratios of m-ZrO_2 are retained due to the long periods of heating and cooling times which

affect the microstructure results; there is a reduced densification of the material.

(iii) *Characterization studies*

Powder X-ray diffraction analysis of the sintered samples was carried out in order to study the structural properties of ZTA nanocomposites using Bruker D8 XRD with a scanning rate of 0.1 s/step. The pelletized samples were polished with 10 μm diamond paste on a rotating disk. Final polishing was done with 3 and 1 μm diamond paste to obtain the mirror polishing with a lapping machine. The surface morphology, EDX analysis and elemental mapping were studied with Hitachi S-3400 SEM. The microstructural characteristics and SAED patterns of ZTA nanocomposites were analyzed by Transmission Electron Microscopy using 200 kV JEOL JEM 3010 HRTEM model with an applied voltage of 200 kV. Thermogravimetric (TG) and Differential Thermal Analysis (DTA) were carried out to study the thermal behavior, phase transition and formation of different phases of 90% Al–10% Zr nanocomposites using EXSTAR TG/DTA 6000 series. The analyses were done in nitrogen atmosphere at a heating rate of 10 °C/min while weight change was recorded as a function of temperature. Apparent porosity and bulk density of the sintered specimens were determined by Archimedes' principle. Initially sintered samples were weighed in dry state and immersed in water and kept under the boiling condition for 8 h to ensure that water is filled up in the open pores completely. Then the suspended weights were calculated. From these values, the apparent porosity and bulk density of different compositions were measured as follows:

Dry weight of the samples $= W_d$

Soaked weight of the samples $= W_s$

Suspended weight of the samples $= W_a$

% Apparent porosity $= ((W_s - W_d)/(W_s - W_a)) \times 100$

Bulk density $= W_d/(W_s - W_a)$

The relative densities of nanocomposites were calculated from the bulk density for different sintering temperatures.

3. Results and discussion

3.1. X-ray diffraction analysis

Fig. 1 shows the X-ray diffraction patterns of $Al_{1-x}Zr_x$ ($x = 5$–20 mol%) nanocomposites. In all samples the rhombohedral (α-Al_2O_3), monoclinic (m-ZrO_2) and tetragonal (t-ZrO_2) phases were observed without any impurity peaks. The phases were matched with the JCPDS data and the lattice parameters of all phases were estimated as shown in Table 1. The presence of α-Al_2O_3 phase was confirmed from (113), (012), (104), (110) and (116) reflections. The existence of m-ZrO_2 phase corresponds to ($\bar{1}11$) and (111) reflections and t-ZrO_2 phase was identified from (101) and (200) reflections.

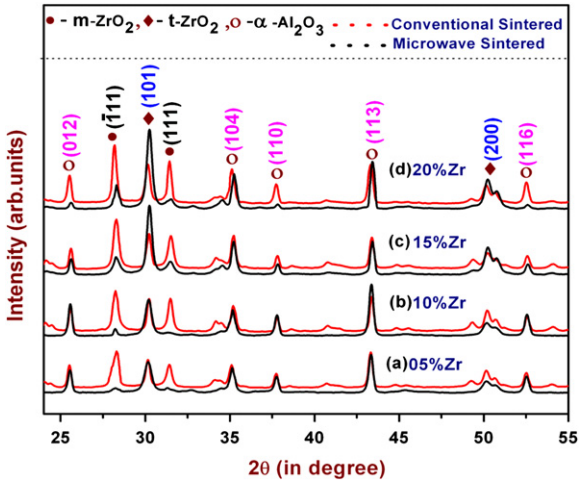

Fig. 1. XRD patterns of $Al_{1-x}Zr_x$ ($x = 5$, 10, 15 and 20 mol%) nanocomposites sintered at 1300 °C by conventional and microwave sintering techniques.

Table 1
Structural parameters of ZTA nanocomposites sintered at 1300 °C.

Phase	Crystal structure	Lattice parameters and angles		
		a/α	*b*/β	*c*/γ
α-Al_2O_3	Rhombohedral	4.758/90	4.758/90	12.991/120
t-ZrO_2	Tetragonal	3.606/90	3.606/90	5.175/90
m-ZrO_2	Monoclinic	5.142/90	5.200/99.205	5.311/90

JCPDS Refs: α-Alumina: (Ref.: 82–1467), t-ZrO_2: (Ref.: 81–1544) and m-ZrO_2: (Ref.: 83–0944).

In the present study, the observed XRD patterns reveal significant variations in the tetragonality of ZrO_2 and the grain size of α-Al_2O_3 with different zirconia contents for samples prepared by both the conventional and microwave sintering methods. Microstructure and mechanical strength of ZTA composites can be determined by the amount of tetragonal ZrO_2 retained in the matrix [6]. The stabilization of tetragonal phase can be ascribed to the particle-size effect. Chandradass and Dong-sik [17] reported that the smaller the particle size of the t-ZrO_2 phase, the more stable it is at low temperature because of its larger specific area. Since the ZrO_2 grains were embedded in alumina matrix, grain growth of zirconia is greatly inhibited.

Figs. 2 and 3 illustrate the peak intensity variations of all phases with respect to different zirconia contents for the samples sintered both by conventional and microwave techniques. The peaks at 28.15°, 30.24° and 43.31° correspond to m-ZrO_2, t-ZrO_2 and α-Al_2O_3 phases respectively. Addition of 5% zirconia into the α-Al_2O_3 matrix shows no formation of monoclinic phase in the microwave sintered sample, whereas an intense crystalline peak of monoclinic phase is observed for the conventional sintered sample as shown in Fig. 3a. However, a slow crystalline growth of m-ZrO_2 phase was observed for higher zirconia content in

the microwave sintered sample. For 5% Zr composition, the t-ZrO_2 phase is almost overlapping in both conventional and microwave sintered samples (Fig. 3b). Further increase in the zirconia content gradually increases the intensity of t-ZrO_2 phase for the microwave sintered sample. The decrease in the t-ZrO_2 phase of the conventional sintered sample may be due to the abnormal grain growth of large m-ZrO_2 grains for the higher content of zirconia. For the microwave sintered samples, larger degree of fine crystallites of t-ZrO_2 was observed, which confirms that the tetragonality is retained in the microwave sintered sample with improved microstructure and densification. Hence it is confirmed that better transformation toughening could be achieved by the microwave sintering method.

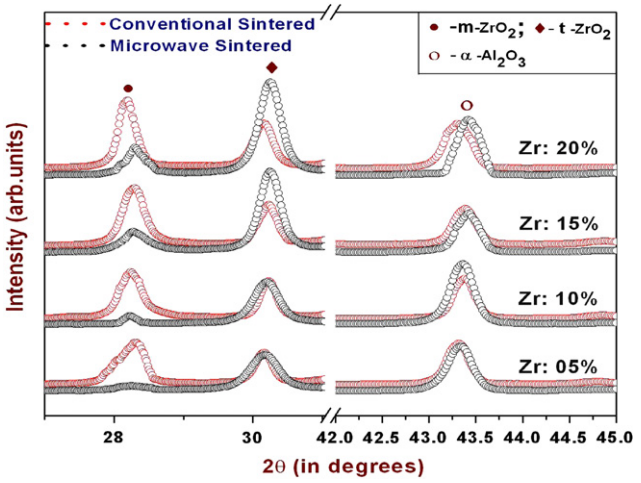

Fig. 2. Peak intensity variations of different phases of ZTA nanocomposites with Zirconia contents (5–20 mol%).

Fig. 3c shows the increase in crystalline growth of α-Al_2O_3 phase with increasing zirconia content (5–20 mol%) for both the sintered materials. However, closer examination reveals that the microwave sintered material exhibits relatively high intense peaks compared to conventional sintered material, which confirms the improved crystallinty. Fig. 3d illustrates the effect of zirconia content on the average grain size of α-Al_2O_3 determined by Scherrer's formula from the FWHM (β) value measured from the peak broadening. It is observed that the average grain size of α-Al_2O_3 gradually decreases with increasing zirconia content. Compared to the conventional sintered material,

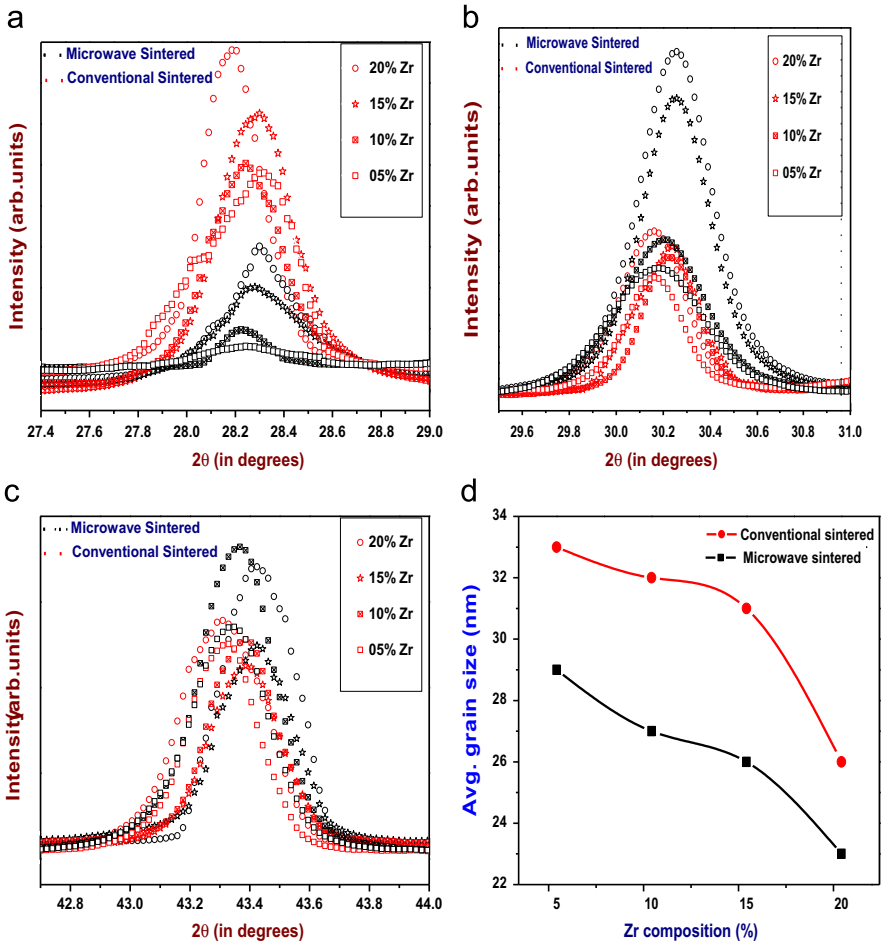

Fig. 3. A composite plot of XRD patterns obtained for $Al_2O_{3-x}ZrO_2$ powder (where x=5, 10, 15 and 20 mol%) sintered at 1300 °C. Peak intensity variations of (a) m-ZrO_2, (b) t-ZrO_2 and (c) α-Al_2O_3 phases for different zirconia contents by both the conventional and microwave sintered samples. (d) Average grain size of α-Al_2O_3 with respect to zirconia content (x=5, 10, 15 and 20 mol%) for both conventional and microwave sintering techniques.

the grain growth of α-Al_2O_3 matrix is greatly inhibited in the microwave sintered sample. The smaller size and uniform distribution of particles in the microwave sintered sample improve the microstructure of the nanocomposites. From the XRD results, it is concluded that the metastable tetragonal phase increases with increasing zirconia content for the microwave sintered sample.

3.2. Scanning electron microscope (SEM) analysis

Fig. 4a and b shows the microstructure of conventional and microwave sintered 90% Al–10% Zr nanocomposites. The micrographs show intergranular fracture with uniform grain size distribution without any observable cracks or pores and abnormal grain growth. The microstructure of conventional sintered sample (Fig. 4a) shows relatively large size particles with some pores at isolated pockets. It is presumed that the voids are nucleated at the grain boundary triple points and grow around the matrix grain. Relatively large voids are created due to the pores, which are originated from entrapped pore in the green compacts and also during sintering. SEM micrograph of microwave sintered ZTA nanocomposites shows relatively finer distribution of particles (Fig. 4b). During sintering, finely dispersed zirconia particles retard the motion of alumina grain boundaries, which inhibit the grain growth of alumina matrix [8,18]. The presence of Al and Zr was confirmed by EDAX analysis as shown in Fig. 4c. Fig. 5 shows the elemental mapping of ZTA nanocomposites carried out on a polished surface. The conventional sintered material shows inhomogeneous particles distribution with some pores in the microstructure (Fig. 5a and b). But it is observed that in the microwave sintered sample, the distributions of Zr and Al are more homogeneous as no part of the micrograph shows clustering of either Zr or Al matrix (Fig. 5c and d) [19].

3.3. Transmission electron microscope (TEM) analysis

Fig. 6a and b illustrates the TEM images of ZTA (90% Al–10% Zr) nanocomposites sintered at 1300 °C by conventional and microwave methods. The TEM results indicate that the synthesized particles have distinctiveness with some particles possessing 'sponge-like' appearance. The micrograph consists of dark batches and fine sized light gray shaded particles of ZrO_2 grains which were embedded into the Al_2O_3 matrix. The samples prepared by conventional sintering possess dark batches of particles in the range of ~100 nm and fine sized shaded light particles of around 60 nm (Fig. 6a). For the microwave sintered

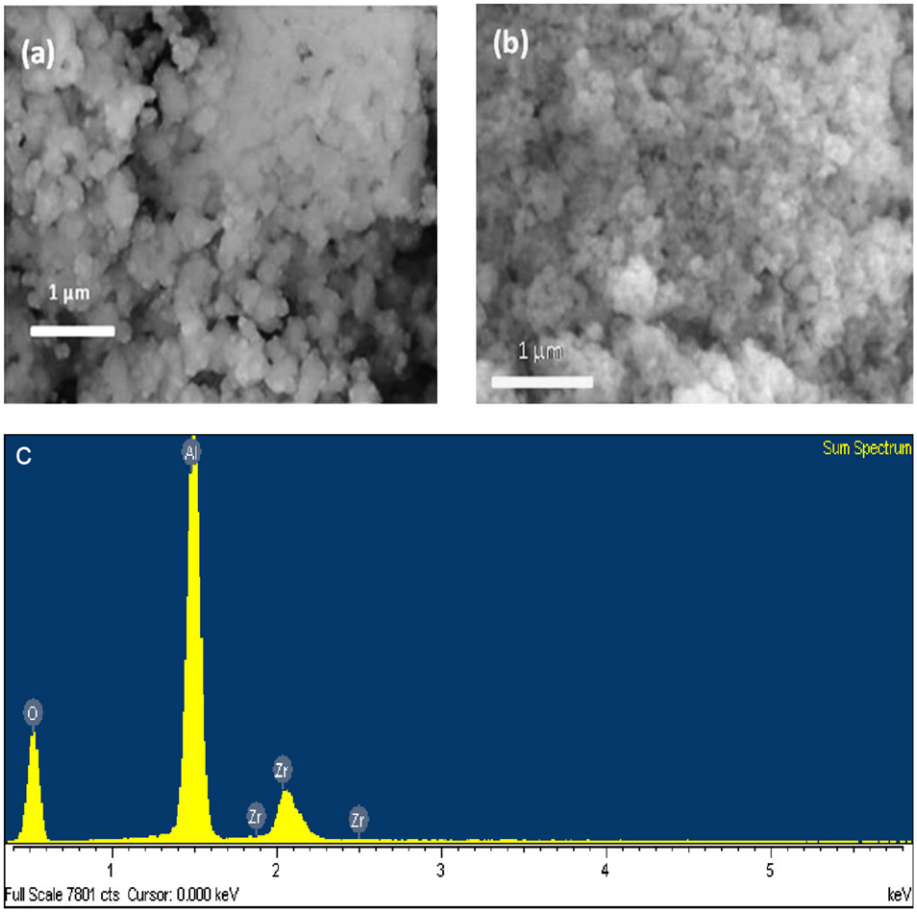

Fig. 4. SEM micrograph of (a) conventional sintered, (b) microwave sintered ZTA (90% Al–10% Zr) nanocomposites at 1300 °C and (c) EDAX spectrum of microwave sintered ZTA (90% Al–10% Zr) nanocomposites at 1300 °C.

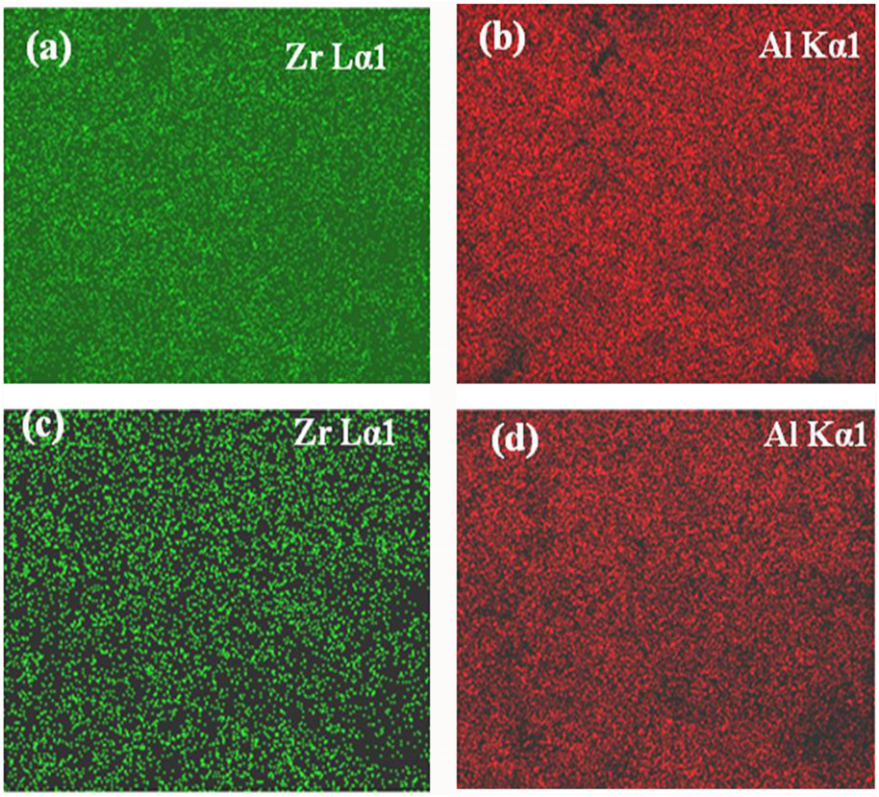

Fig. 5. Elemental mapping of (a) and (b) conventional and (c) and (d) microwave sintered ZTA nanocomposites at 1300 °C.

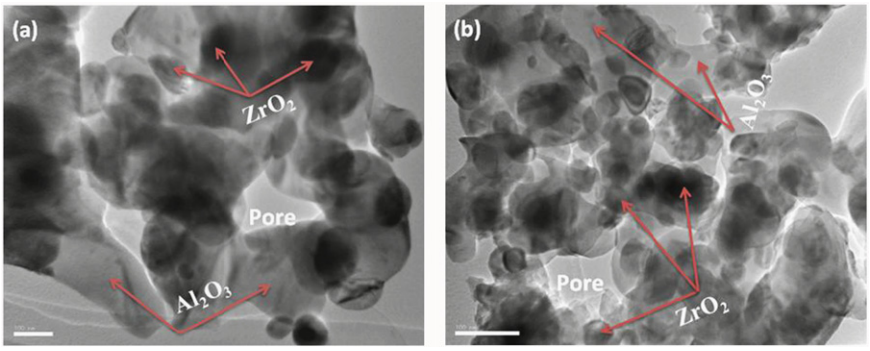

Fig. 6. TEM images (100 nm resolution) of (a) conventional (b) microwave sintered ZTA nanocomposites at 1300 °C.

sample the average particle size of dark and shaded light particles was observed as ~50 nm and ~30 nm respectively (Fig. 6b). In the micrographs, some discrete tiny pores of about ~120 nm were also observed along with dense particles, similar results were reported for the conventional sintered ZTA material [20].

The HR-TEM images show differences in lattice fringe patterns for the conventional and microwave sintered ZTA samples as shown in Fig. 7a and b. The microstructure shows larger grain size and distinct bimodal distribution for the conventional sintered samples. From the lattice fringe patterns, the interplanar spacing was measured to be 0.520 nm for the conventional sintered sample. Relatively fine grains and monomodal distribution of particles were observed for the microwave sintered sample with reduced interplanar spacing of $d=0.335$ nm [21]. Fig. 7c and d shows the selected area electron diffraction (SAED) pattern of conventional and microwave sintered ZTA nanocomposites. The results show that the irregular periodic arrangement of atoms was observed from the conventional sintered sample. For the microwave sintered sample the atoms are periodically arranged in the entire lattice; this result indicates that the conventional sintered sample possesses reduced crystallinity compared to the microwave sintered sample.

3.4. Thermal analysis

TG-DTA curve of ZTA nanocomposites is shown in Fig. 8. In the temperature range RT-110 °C, a broad endothermic

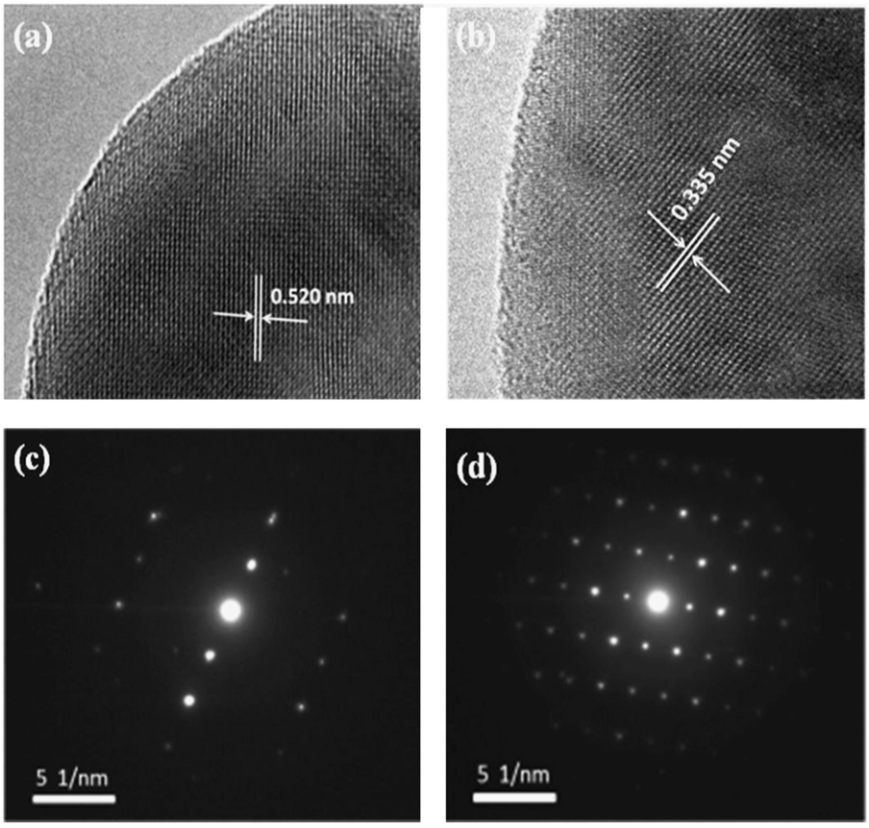

Fig. 7. (a) and (b) HR-TEM images and (c) and (d) SAED patterns of conventional and microwave sintered ZTA specimens.

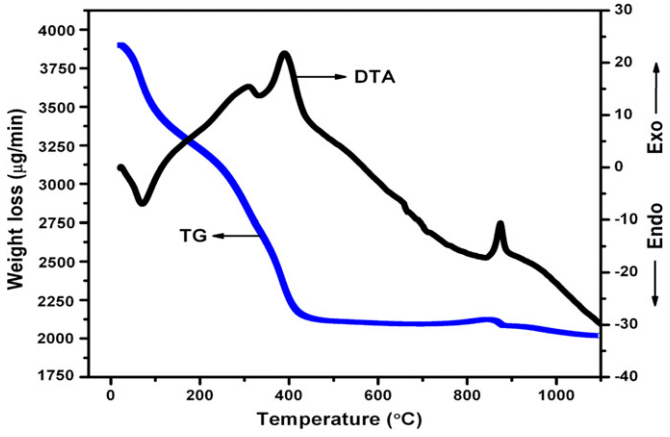

Fig. 8. TG-DTA curves of 90% Al–10% Zr nanocomposites.

peak appeared around 70 °C with a weight loss of 12.5% which is associated with the dehydroxylation of pseudoboehmite due to the vaporization of physically bounded adsorbed methoxy–ethanol. In this temperature range, the powder contains disordered pseudoboehmite at room temperature with more than 15% excess solvent [9]. The theoretical weight loss due to dehydroxylation of pseudoboehmite is about 13% for the above composition, and hence the experimental observations very well agree with the theoretical results. The small exothermic peak at 310 °C may be due to the crystallization of γ-Al_2O_3 from Boehmite ($Al(OH)_3$). In the reaction AlO(OH) first transforms to an amorphous alumina on dehydroxylation, which subsequently crystallizes to γ-Al_2O_3. The second maximal exothermic peak at 400 °C is assigned to the crystallization of cubic-ZrO_2 from $Zr(OH)_4$. The gradual weight loss of about 27% was observed in the range 240–430 °C, which agrees with the theoretical weight loss of 28%. In this region, the Boehmite ($Al(OH)_3$) decomposes with the formation of γ-Al_2O_3 according to the reaction:

$$Al(OH)_3 = AlO(OH) + H_2O \quad (1)$$

$$2AlO(OH) = Al_2O_3 + H_2O \quad (2)$$

The transformation of $Zr(OH)_4$ to cubic ZrO_2 is based on the reaction:

$$Zr(OH)_4 = ZrO_{1.5}(OH) + 1.5H_2O \quad (3)$$

$$ZrO_{1.5}(OH) = ZrO_2 + 0.5H_2O \quad (4)$$

At higher temperature, another exothermic peak was observed at around 875 °C, due to the phase transformation of tetragonal ZrO_2 from cubic ZrO_2. The corresponding weight loss (1.5%) agrees with the 2% theoretical weight loss. The results reveal the phase transition of α-Al_2O_3 from bayerite ($Al(OH)_3$) and boehmite (Al(O)OH) phases as well as the crystallization of zirconia from an amorphous zirconium hydroxide [7].

Table 2
Apparent porosity and bulk density of $Al_{1-x}Zr_x$ ($x=5$, 10, 15 and 20 mol%) nanocomposites for different sintering temperatures.

Zirconia composition (%)	Sintered at 1300 °C				Sintered at 1450 °C			
	Apparent porosity (%)		Bulk density (g/cc)		Apparent porosity (%)		Bulk density (g/cc)	
	Conventional	Microwave	Conventional	Microwave	Conventional	Microwave	Conventional	Microwave
5	13.87	14.21	3.48	3.43	1.32	1.31	3.82	3.85
10	16.92	11.51	3.47	3.56	2.07	1.22	3.86	4.05
15	18.10	8.71	3.52	3.69	2.85	1.05	3.95	4.12
20	20.40	3.14	3.53	3.78	4.19	0.74	3.91	4.27

3.5. Density measurements

The apparent porosity and bulk density values of the samples prepared by conventional sintering and microwave sintering for two different sintering temperatures are listed in Table 2. It is observed that the apparent porosity and bulk density vary with zirconia content. The apparent porosity of the microwave sintered samples gradually decreases with increasing zirconia content. But the apparent porosity increases for the conventional sintered samples; however there is no gradual increase in the relative density or a considerable reduction in the relative density with increasing temperature as well as increasing of Zr content could be observed i.e., the total relative density is increased with respect to two different sintering temperatures but when considering the different Zr contents it shows a decreasing nature and this shows that the porosity is not influencing a huge change in the relative density of the material, rather only there is a considerable change. The porosity reduction was observed up to 3.14% and 0.74% for the microwave sintered material at 1300 °C and 1450 °C respectively and the reduction in the entrapped porosity may be due to the increasing finer tetragonal grains in the matrix, which can pin the grain boundary diffusion. For the conventional sintered sample, the higher degree of large grains of m-ZrO_2 could not pin the grain boundary diffusion, and hence reflected in the inhomogeneity of the microstructure, which is against the densification of the material. In addition the relative fast grain growth rate has a detrimental effect on the density of the conventional sintered samples because of exaggerated ZrO_2 coarsening and pore coalescence. The bulk density increases with increasing zirconia content for the microwave sintered samples, while it decreases for the conventional sintered material, which is due to the apparent porosity of the sintered compacts. The maximum bulk density of 4.27 gm/cc was obtained for the microwave sintered sample at 1450 °C for higher content of zirconia. The results confirm that the percentage of tetragonal phase retention is more for higher content of zirconia in the microwave sintered sample, moreover when increasing the zirconia content the microwave absorption efficiency was also increased which leads to higher densification. i.e., the zirconium exhibits strong absorption to microwave power

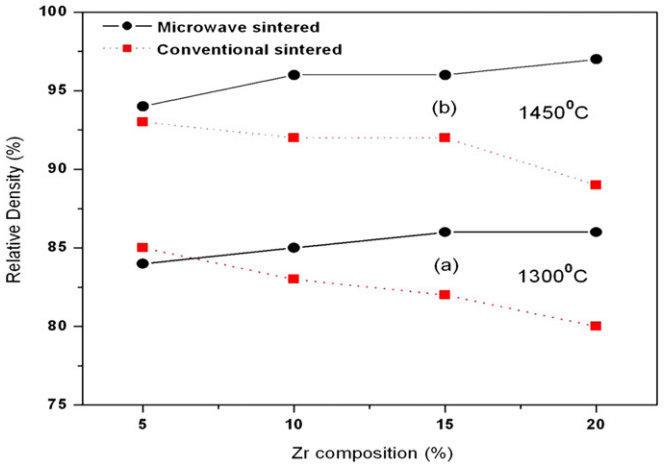

Fig. 9. Relative density of $Al_2O_{3-x}ZrO_2$ ($x=5$, 10, 15, 20 mol%) nanocomposites prepared by conventional and microwave sintering at (a) 1300 °C and (b) 1450 °C.

than the alumina matrix. It shows within short heating and holding time that the microwave technique could sinter the material at elevated temperature than the conventional sintering and it resembles the time–temperature profile. Reduction in t-ZrO_2 phase in conventional sintered samples shows poor density.

The relative densities of $Al_2O_{3-x}Zr_xO_2$ ($x=5$, 10, 15, 20 mol%) nanocomposites were calculated from the bulk density for different sintering temperatures for both the microwave and conventional sintered specimens as shown in Fig. 9. The material sintered at 1300 °C exhibits low densification of about 80–87%. The porosity in the material usually originates from the entrapped pore during green compaction and the elimination of hydrated water from the additive. It is very difficult to remove the pores during the final stage of sintering at low temperature, which confers low sintered density. The rate of densification increases with further increase in the sintering temperature and better densification is achieved at 1450 °C [22]. The maximum theoretical density of 97% can be achieved with addition of 20 mol% of ZrO_2 at 1450 °C in the microwave sintered material.

In the conventional sintered sample the relative density gradually decreases with increasing zirconia content (5–20 mol%) at the same sintering conditions due to the

considerable increase in the monoclinic phase. The monoclinic phase usually possesses large grains compared to the tetragonal phase, which leads to an abnormal grain growth for higher zirconia content (20 mol%). This confirms that the monoclinic phase reduces the densification of the material for higher zirconia content as well as promotes the grain growth [11]. The smaller unit cell volume of the tetragonal phase usually denser than the monoclinic phase is responsible for the densification of the material. For the conventional sintered material, t→m phase transformation of zirconia causes volume expansion of about ~5% leading to a decrease in the relative density of the composites. The decrease in t-ZrO_2 phase and increase in m-ZrO_2 phase may be explained by the rapid increase in the grain size of material. Since Al_2O_3–ZrO_2 composites were prepared from unstabilized ZrO_2, cooling from higher temperature causes spontaneous t→m phase transformation. This induces severe micro-cracking, which probably leads to lower density for the sintered sample even though the green density is higher. This reduction may also occur because of the agglomeration of zirconia grains, which could not be controlled during sintering. These agglomerates lead to the formation of coarse zirconia grains. The density of the microwave sintered material increases with increasing zirconia content for both the sintering temperatures due to the considerable increase in the tetragonal phase. The results reveal that the mechanical properties of ZTA nanocomposites can be improved by the microwave sintering.

4. Conclusion

The sol–gel prepared ZTA nanocomposites with different zirconia contents (5–20 mol%) were sintered by conventional and microwave techniques. The effect of microwave sintering on the structural and mechanical properties has been systematically studied. It is observed that the mean particle size of Al_2O_3 matrix decreases with increasing zirconia content in the microwave sintered material, which leads to the improved microstructure and densification of the material. The transformation toughening of the ZTA nanocomposites largely depends on the retention of t-ZrO_2 at room temperature and thus the microwave sintered material exhibits large volume fraction of t-ZrO_2 retention. The surface morphology shows fine particle size distribution with less degree of porosity for the microwave sintered material. The reduction in the interplanar spacing is observed for the microwave sintered materials and the grain boundaries are completely free from amorphous phase. This leads to high purity retention of phases even after high temperature sintering with improved crystallinity. Maximum theoretical density of about 97% could be achieved for the microwave sintered sample for higher zirconia content. The results reveal that microwave sintering is effective in improving the microstructure and density of ZTA nanocomposites, which will be useful for high temperature structural ceramic applications.

Acknowledgment

The authors would like to thank Dr. Ajayan Vinu, Senior Researcher, National Institute for Materials Science (NIMS), Japan, for extending the SEM and HR-TEM facilities.

References

[1] Vladimir V. Srdic, L. Radonjic, Transformation toughening in sol–gel derived Alumina–Zirconia composites, Journal of the American Ceramic Society 80 (8) (1997) 2056–2060.
[2] V. Srdic, L. Radonjic, Seeded sol–gel derived Alumina–Zirconia composites, Ceramics International 21 (1995) 5–11.
[3] A. Taavoni-Gilan, E. Taheri-Nassaj, H. Akhondi, The effect of zirconia content on properties of Al_2O_3–ZrO_2 (Y_2O_3) composite nanopowders synthesized by aqueous sol–gel method, Journal of Non-Crystalline Solids 355 (2009) 311–316.
[4] Richard H.J. Hannink, Patrick M. Kelly, Barry C. Muddle, Transformation toughening in Zirconia-containing ceramics, Journal of the American Ceramic Society 83 (3) (2000) 87–461.
[5] Xue-Jun Jin, Transformation toughening in Zirconia-containing ceramics, Current Opinion in Solid State and Materials Science 9 (2005) 313–318.
[6] J. Wang, R. Stevens, Zirconia-toughened alumina (ZTA) ceramics, Journal of Materials Science 24 (1989) 3421–3440.
[7] P. Rana Raghunath, K. Pratihar Swadesh, Santanu Bhattacharyya, Effect of powder treatment on the crystallization behavior and phase evolution of Al_2O_3–high ZrO_2 nanocomposites, Journal of Materials Science 41 (2006) 7025–7032.
[8] D. Sarkar, S. Adak, N.K. Mitra, Preparation and characterization of an Al_2O_3–ZrO_2 nanocomposites, Part I: powder synthesis and transformation behavior during fracture, Composites Part A 38 (2007) 124–131.
[9] J. Chandradass, Jae Hong Yoon, Dong-sik Bae, Synthesis and characterization of zirconia doped alumina nanopowder by citrate–nitrate process, Materials Science and Engineering: A 473 (2008) 360–364.
[10] P. Rana Raghunath, K. Pratihar Swadesh, Santanu Bhattacharyya, Powder processing and densification behavior of alumina–high zirconia nanocomposites using chloride precursors, Journal of Materials Processing Technology 190 (2007) 350–357.
[11] Yinping Ye, Jiangong Li, Huidi Zhou, Jiamin Chen, Microstructure and mechanical properties of yttria-stabilized ZrO_2/Al_2O_3 nanocomposites ceramics, Ceramics International 34 (2008) 1797–1803.
[12] Dinesh K. Agrawal, Microwave processing of ceramics, Current Opinion in Solid State and Materials Science 3 (1998) 480–485.
[13] Morteza Oghbaei, Omid Mirzaee, Microwave versus conventional sintering: a review of fundamentals, advantages and applications, Journal of Alloys and Compounds 494 (2010) 175–189.
[14] R.R. Menezes, R.H.G.A. Kiminami, Microwave sintering of alumina–zirconia nanocomposites, Journal of Materials Processing Technology 203 (2008) 513–517.
[15] J. Samuels, J.R. Brandon, Effect of composition on the enhanced microwave sintering of alumina-based ceramic composites, Journal of Materials Science 27 (1992) 3259–3265.
[16] E.T. Thostenson, T.W. Chou, Microwave processing: fundamentals and applications, Composites Part A: Applied Science and Manufacturing 30 (1999) 1055–1071.
[17] J. Chandradass, Dong-sik Bae, Nano α-Al_2O_3–t-ZrO_2 composite powders by calcining an emulsion precursor at 1100 °C, Journal of Alloys and Compounds 469 (2009) L10–L12.

[18] D. Sarkar, S. Adak, M.C. Chu, S.J. Cho, N.K. Mitra, Influence of ZrO_2 on the thermo-mechanical response of nano-ZTA, Ceramics International 33 (2007) 255–261.
[19] Sarkar Debasish, Mohapatra Deepak, Sambarta Ray, Santanu Bhattacharyya, Adak Sukumar, Mitra Niren, Synthesis and characterization of sol–gel derived ZrO_2 doped Al_2O_3 nanopowder, Ceramics International 33 (2007) 1275–1282.
[20] Jae-Kil Han, Fumio Saito, Byong-Taek Lee, Microstructures of porous Al_2O_3–50 wt% ZrO_2 composites using in-situ synthesized Al_2O_3–ZrO_2 composite powders, Materials Letters 58 (2004) 2181–2185.
[21] D.D. Upadhyaya, A. Ghosh, G.K. Dey, R. Prasad, A.K. Suri, Microwave sintering of zirconia ceramics, Journal of Materials Science 36 (2001) 4707–4710.
[22] Lee Ki-Yong, E.D. Case, Microwave sintering of alumina matrix zirconia composites using a single-mode microwave cavity, Journal of Materials Science 18 (1999) 201–203.